

ELECTRONIC SUPPORTING INFORMATION

Heteroleptic Cu(II)-polypyridyl complexes as photonucleases

Vikram Singh,^{a,b} Kumkum Sharma,^a Bhaskaran Shankar,^a Satish Kumar Awasthi,^a
Rinkoo Devi Gupta^{*c}

^a Department of Chemistry, University of Delhi, Delhi-110 007, India.

^bDepartment of Chemical Engineering, Pohang University of Science and Technology, Pohang-
790-784, South Korea.

^cFaculty of Life Sciences and Biotechnology, South Asian University, Delhi-110 021, India

Email: rdgupta@sau.ac.in

Synthesis of TPY-1 to 3.^[1-3] 0.33 g (8.24 mmol) of NaOH was crushed and added to 6 mL of PEG-300 and stirred to form a suspension. To this was added, 0.96 mL (8.24 mmol) of 2-acetylpyridine and further stirred for 20 minutes. 4.12 mmol of respective aldehyde was then added to the reaction mixture and kept in ice bath at 0 °C for 2 h with constant stirring. Gradually, the suspension became thick and occasional manual stirring was employed. After 2 h, 5 mL of 30% aq. NH₃ solution was added and the suspension was heated at 100 °C for 2 h. A yellowish precipitate formed during refluxing was isolated by vacuum filtration and washed with H₂O and cold ethanol (10 mL) and dried under vacuum. The crude product was recrystallized with ethanol. Yield: ~ 40-50%. **TPY-1:** ¹H NMR (400 MHz, CDCl₃): δ 8.73 (d, *J* = 4.75 Hz, 2H⁷); δ 8.71(s, 2H⁵); δ 8.69 (d, *J* = 5 Hz, 2H¹); δ 8.63 (d, *J* = 8 Hz, 2H⁴); δ 7.85 (dt, *J* = 6 Hz, *J* = 8 Hz, *J* = 2 Hz, 2H³); δ 7.75 (d, *J* = 4.75 Hz, 2H⁶); δ 7.33 (dd, *J* = 6 Hz, *J* = 1.2 Hz, *J* = 4.75 Hz, 2H²). **TPY-2:** ¹H NMR (400 MHz, CDCl₃): δ 8.89 (s, 2H⁵); δ 8.76 (d, *J* = 4.75 Hz, 2H¹); δ 8.72 (d, *J* = 7.9 Hz, 2H⁴); δ 8.43 (s, 1H¹⁰); δ 7.93 (m, 1H⁶ + 1H⁷ + 2H⁸ + 2H⁹); δ 7.52 (m, 2H²); δ 7.36 (m, 2H³). **TPY-3:** ¹H NMR (400 MHz, CDCl₃): δ 8.87 (d, *J* = 8 Hz, 2H⁴); δ 8.75 (d, *J* = 4 Hz, 2H¹); δ 8.59 (s, 2H⁵); δ 8.55 (s, 1H¹⁰); δ 8.05 (m, 2H³ + 2H⁶); δ 7.65 (d, *J* = 9 Hz, 2H⁷); δ 7.40 (m, 2H² + 2H⁸ + 2H⁹). (fig. S1 to S3 for ¹H NMR of TPY-1 to 3).

Synthesis of TPY-4.^[4] Step 1: 8.24 mmol of 2-Acetylpyridine was dropwise added to a suspension of 8.24 mmol crushed NaOH in 45 mL of anhydrous ethanol under N₂ atmosphere. 0.97 g (4.12 mmol) of 1-pyrene caboxaldehyde in 15 mL ethanol was then added to the reaction mixture and stirred constantly for 20 h. The resulting precipitate was filtered and washed with cold ethanol.

Step 2: 0.3 mL (2.68 mmol) of 2-acetyl pyridine was added to a stirred solution of 0.49 g (4.36 mmol) potassium *tert.* butoxide in 60 mL of anhydrous THF. The resulting solution was stirred for 3 h at room temperature under inert atmosphere of N₂ gas. During this time, colour of the solution changes to red. To this solution, 0.68 g (2.04 mmol) of 3-(pyren-1-yl)-1-(pyridin-2-yl)prop-2-en-1-one was added

and stirring was continued overnight. The solution turned deep red and 3.37 g (43.2 mmol) of ammonium acetate along with 60 mL of ethanol were added to it and mixture was refluxed for 5 h. The solvent was removed *in vacuo* and residue was taken in DCM/H₂O mixture and the organic layer was separated. Further, it was dried over anhydrous sodium sulphate and recrystallized by dissolving in minimum amount of CHCl₃ and slowly adding methanol to the hot solution. Yield: ~43 %. ¹H NMR (400 MHz, CDCl₃): δ 8.70 (s, 2H⁵), δ 8.69 (d, *J* = 7.2 Hz, 2H⁴), δ 8.62 (d, *J* = 4.1 Hz, 2H¹), δ 8.07 (m, 1H⁶ + 1H⁷ + 2H⁸ + 2H⁹ + 2H¹⁰ + 1H¹¹), δ 7.89 (td, *J* = 7.2 Hz, *J* = 1.5 Hz, 2H³), 7.29 (ddd, *J* = 7.2 Hz, *J* = 4.1 Hz, *J* = 1.0 Hz, 2H²). (fig. S4 for ¹H NMR of TPY-4)

Synthesis of IMI-1.^[5,6] 0.15 g (0.714 mmol) of 1,10-phenanthroline-5,6-dione and 1.75 g (22 mmol) of NH₄OAc were taken and refluxed at 80 °C until the mixture dissolves. Then, 0.714 mmol of 4-pyridine carboxaldehyde in 7 mL of glacial acetic acid was added to the hot solution. The colour changed to deep red while addition and refluxed for further 3 h. The solution was cool down to room temperature, neutralized by 30 % aq. NH₃ solution during which a yellow precipitate was observed. The precipitate was filtered, washed with cold H₂O and dried *in vacuo*. Yield: ~51%. ¹H NMR (400 MHz, DMSO-*d*₆): δ 9.17 (m, 2H¹); δ 8.90 (m, 2H³ + 2H⁵); δ 8.23 (m, 2H⁴); δ 7.95 (m, 2H²). (fig. S5 for ¹H NMR of IMI-1).

Synthesis of TPYC-1 to TPYC-4. 74 mg (0.02 mmol) of Cu(ClO₄)₂.6H₂O was dissolved in 10 mL of MeOH/CHCl₃ (1:1, v/v) at room temperature. To the stirred solution, added drop-wise 0.02 mmol of respective TPY ligand in 10 mL of MeOH/CHCl₃ (1:4, v/v). The solution was stirred for 2 h and then 59.4 mg (0.02 mmol) of IMI-1 in 10 mL of MeOH/CHCl₃ (4:1, v/v) was added dropwise to the stirred solution. Further stirring for 1 h afforded a light to dark green colored precipitate. The precipitate was washed with

ether and dried over anhydrous calcium chloride and kept in glovebox. Yield: ~ 40-55 %.

Characterization Data for the Complexes.

TPYC-1: ATR-IR (ν_{\max} , cm^{-1}): 2976 (w) (aromatic C-H), 1608 (m) (C=C), 1562 (m) (C=N), 1480, 1076 (vs) (Cl-O stretch), 864 (m), 774 (m). UV-vis (10^{-5} M in CH_3CN) (λ_{\max} , $\log\epsilon$): 275 nm, 4.86; 324 nm, 4.69; 381 nm, 3.85; 744 nm, 1.81. ESI-MS: m/z 356 [$(\text{M}^{2+} - 2\text{ClO}_4)/2$]. $\frac{1}{2}$ CH_3CN (fig. S6). Elemental analysis (%) found (calculated): C: 52.02(52.4); H: 2.61(2.90); N: 14.21(14.49).

TPYC-2: ATR-IR (ν_{\max} , cm^{-1}): 3081 (w) (aromatic C-H), 1608 (m) (aromatic C-H), 1476 (m) (C=N), 1082 (vs) (Cl-O stretch), 791 (m), 730 (m). UV-vis (10^{-5} M in CH_3CN) (λ_{\max} , $\log\epsilon$): 225 nm, 5.03; 279 nm, 4.97; 323 nm, 4.76; 607 nm, 2.36. ESI-MS: m/z 360 ($\text{M} + \text{H}$)⁺ [$\text{M}^+ = (\text{M}^{2+} - 2\text{ClO}_4)/2$] (fig. S7). Elemental analysis (%) found (calculated): C: 55.85(56.19); H: 2.85(3.07); N: 12.01(12.19).

TPYC-3: ATR-IR (ν_{\max} , cm^{-1}): 3076 (w) (aromatic C-H), 1664 and 1605 (m) (C=C), 1475 (m) (C=N), 1079 (vs) (Cl-O stretch), 792 (m), 736 (m). UV-vis (10^{-5} M in CH_3CN) (λ_{\max} , $\log\epsilon$): 248 nm, 4.93; 284 nm, 4.30; 329 nm, 4.20; 671 nm, 1.73. ESI-MS: m/z 385 ($\text{M}^{2+} - 2\text{ClO}_4)/2$ (fig. S8). Elemental analysis (%) found (calculated): C: 57.89(58.24); H: 2.89(3.12); N: 11.29(11.56).

TPYC-4: ATR-IR (ν_{\max} , cm^{-1}): 2963 (w) (aromatic C-H), 1603 (m) (C=C), 1477 (m) (C=N), 1092 (vs) (Cl-O), 852 (m), 796 (w). UV-vis (10^{-5} M in CH_3CN) (λ_{\max} , $\log\epsilon$): 235 nm, 4.73; 268 nm, 4.54; 330 nm, 4.39; 412 nm (sh), 3.90; 594 nm, 1.84. ESI-MS: m/z 397 ($\text{M}^{2+} - 2\text{ClO}_4)/2$ (fig. S9). Elemental analysis (%) found (calculated): C: 58.94(59.25); H: 2.74(3.04); N: 10.92(11.28). (fig. S6 to S9 for ESI-MS of TPYC-1 to 4).

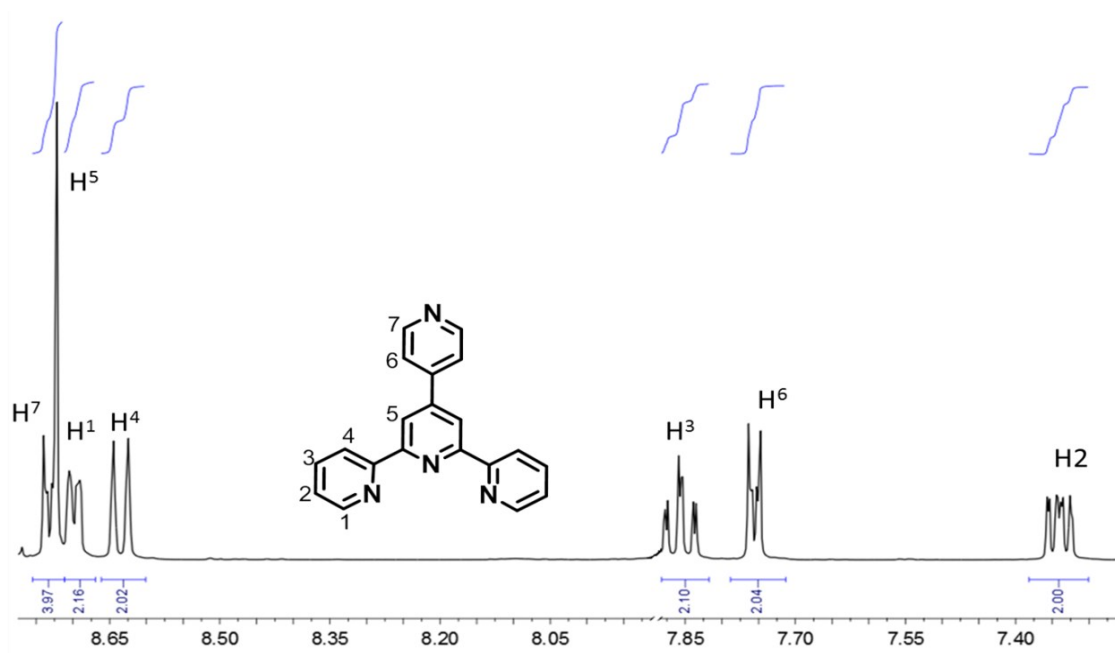


Figure S 1: ^1H NMR spectrum of ligand TPY-1 in CDCl_3 .

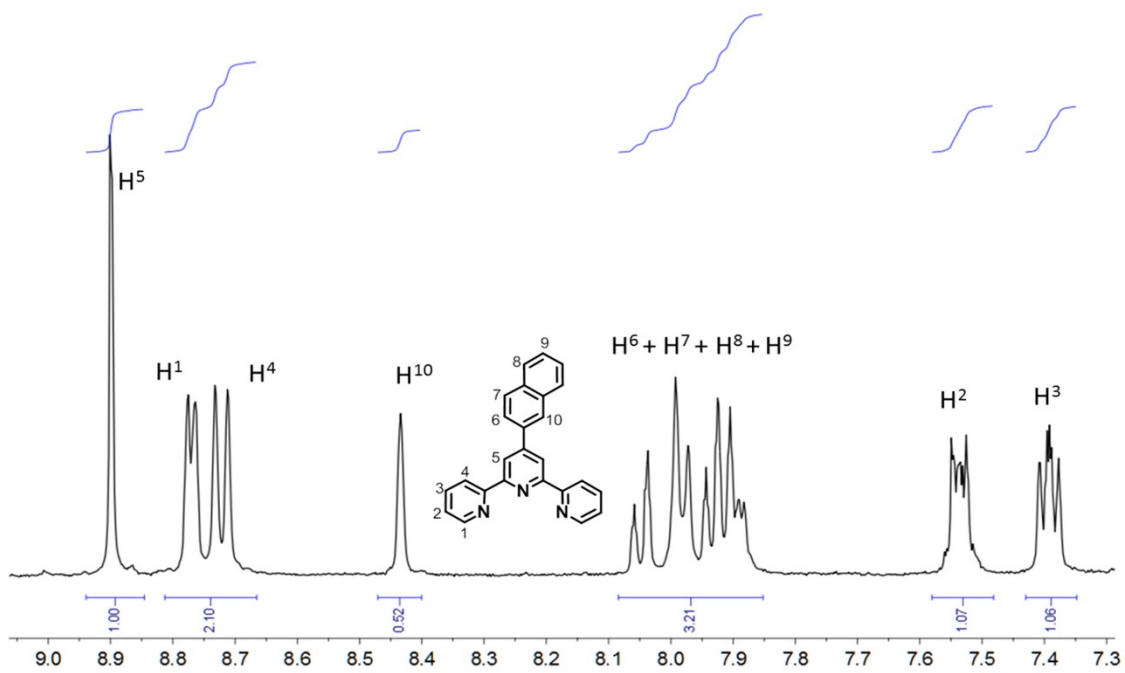


Figure S 2: ^1H NMR spectrum of ligand TPY-2 in CDCl_3 .

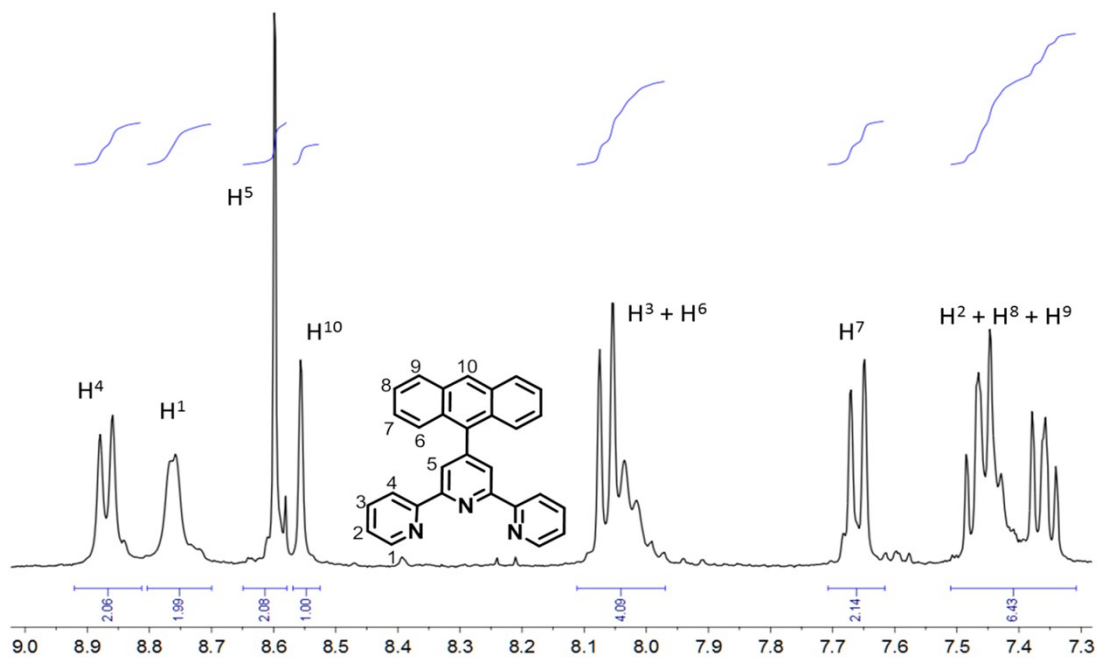


Figure S 3: ^1H NMR spectrum of ligand TPY-3 in CDCl_3 .

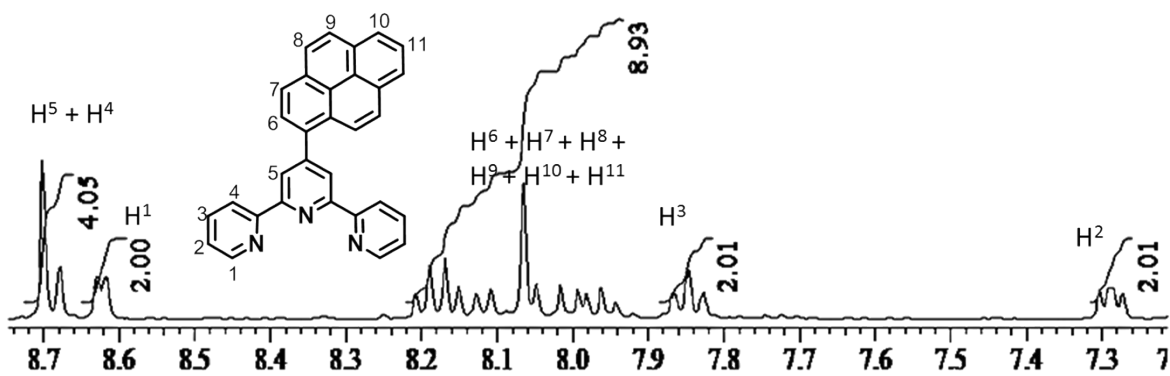


Figure S 4: ^1H NMR spectrum of ligand TPY-4 in CDCl_3 .

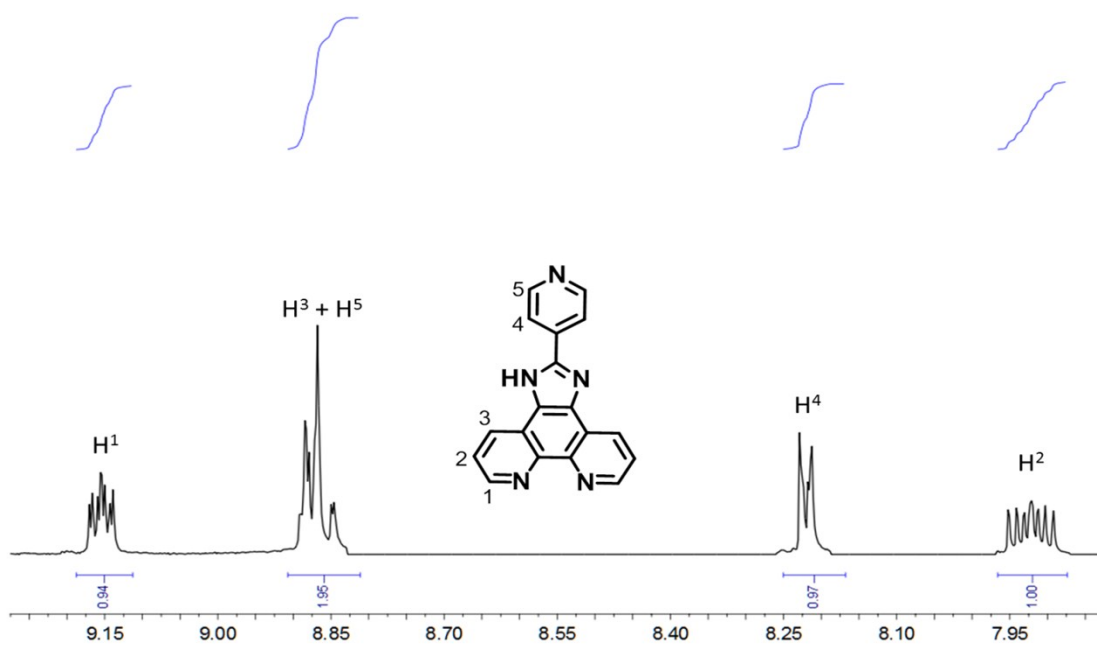


Figure S 5: ¹H NMR spectrum of ligand IMI-1 in deuterated DMSO.

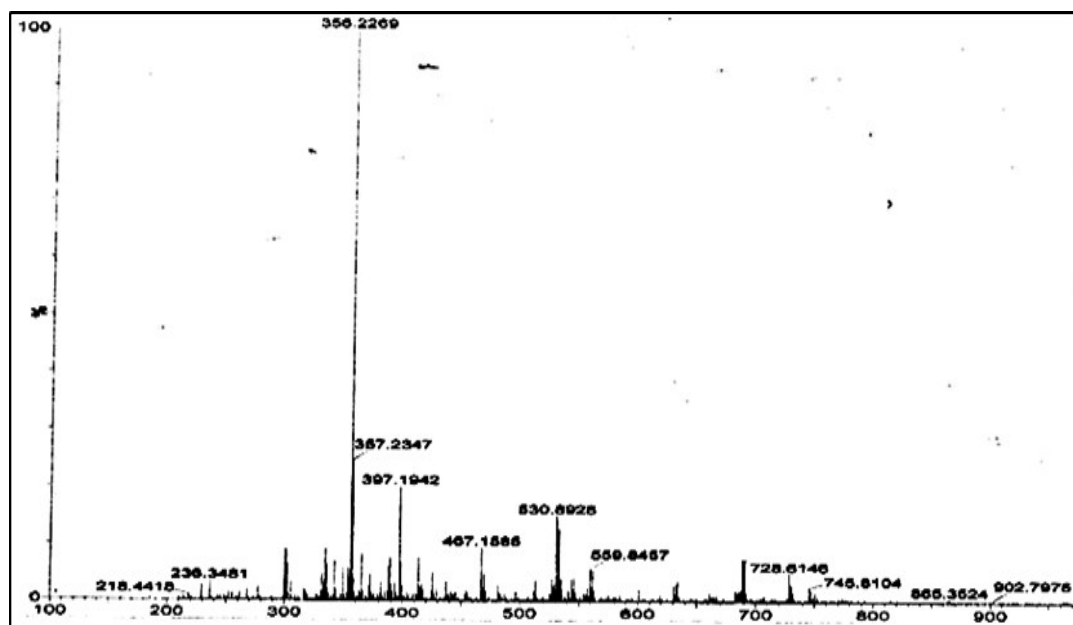


Figure S 6: ESI-MS (+ve mode) of TPYC-1 in CH₃CN. $m/z = 356 (M^{2+} - 2ClO_4)/2$. $\frac{1}{2}$ CH₃CN.

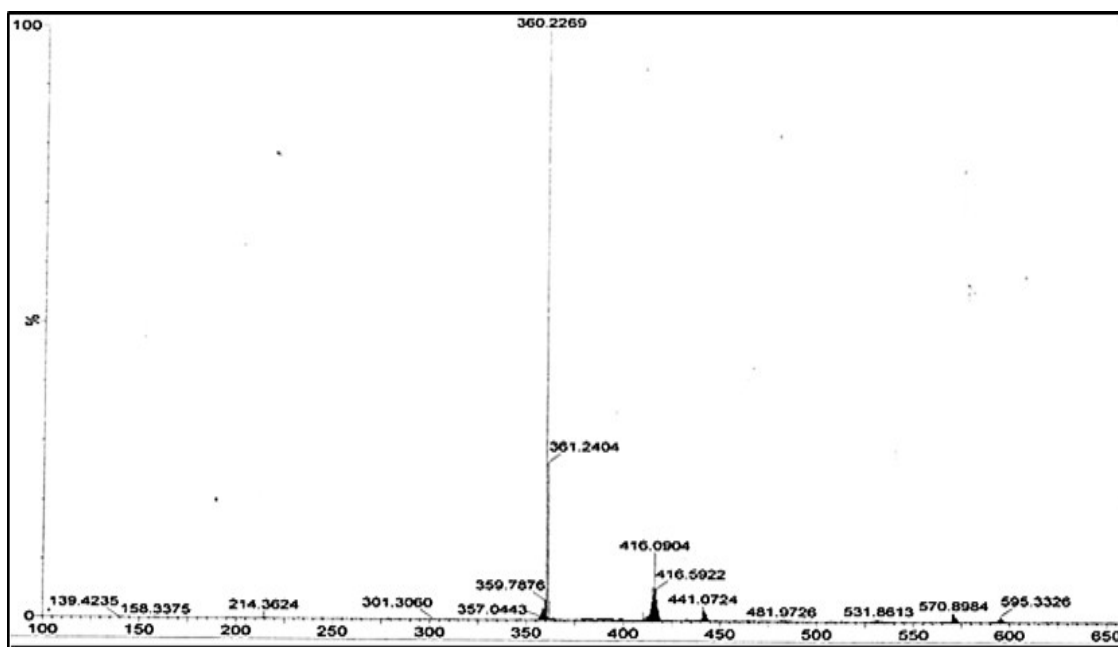


Figure S 7: ESI-MS (+ve mode) of TPYC-2 in CH₃CN. $m/z = 360 (M^{2+} - 2ClO_4)/2$.

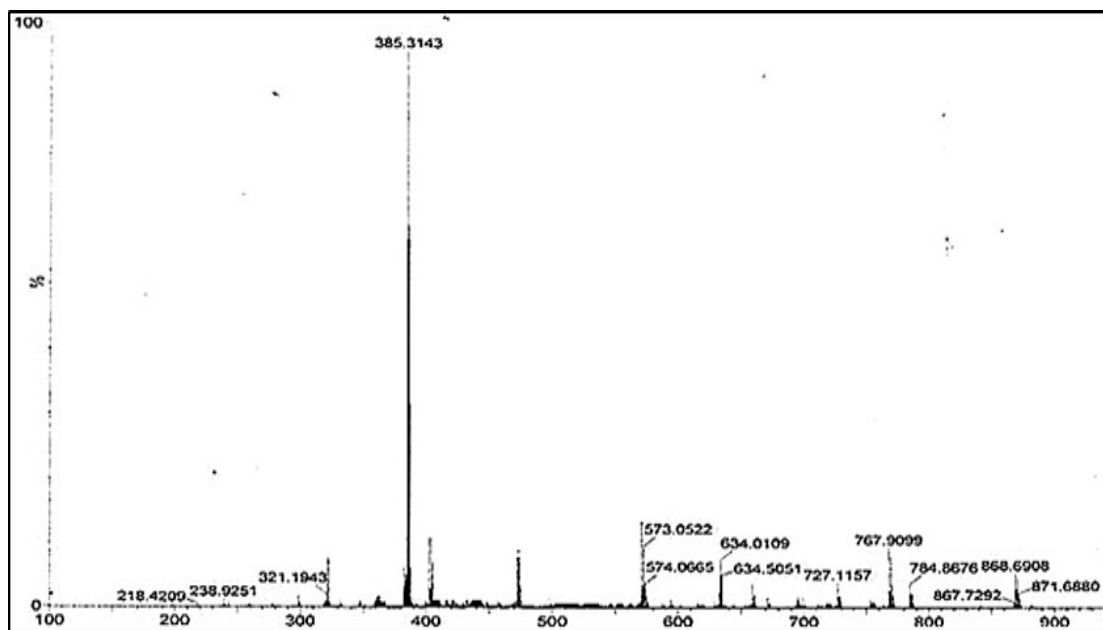


Figure S 8: ESI-MS (+ve mode) of TPYC-3 in CH₃CN. $m/z = 385 (M^{2+} - 2ClO_4)/2$.

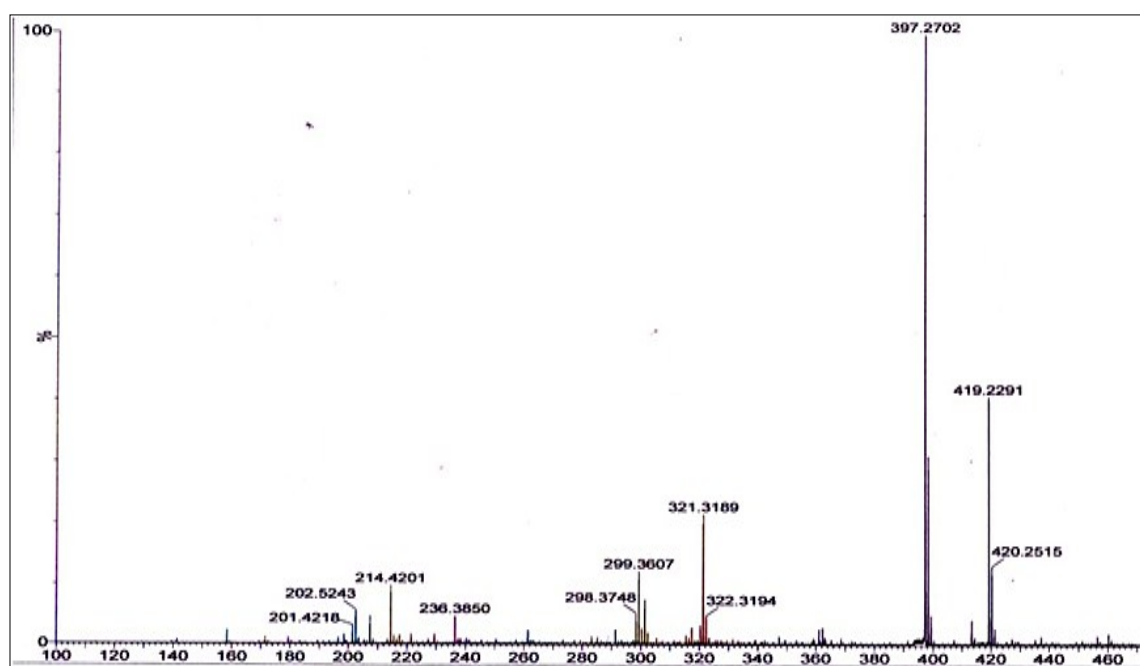


Figure S 9: ESI-MS (+ve mode) of TPYC-4 in CH₃CN. $m/z = 397 (M^{2+} - 2ClO_4)/2$.

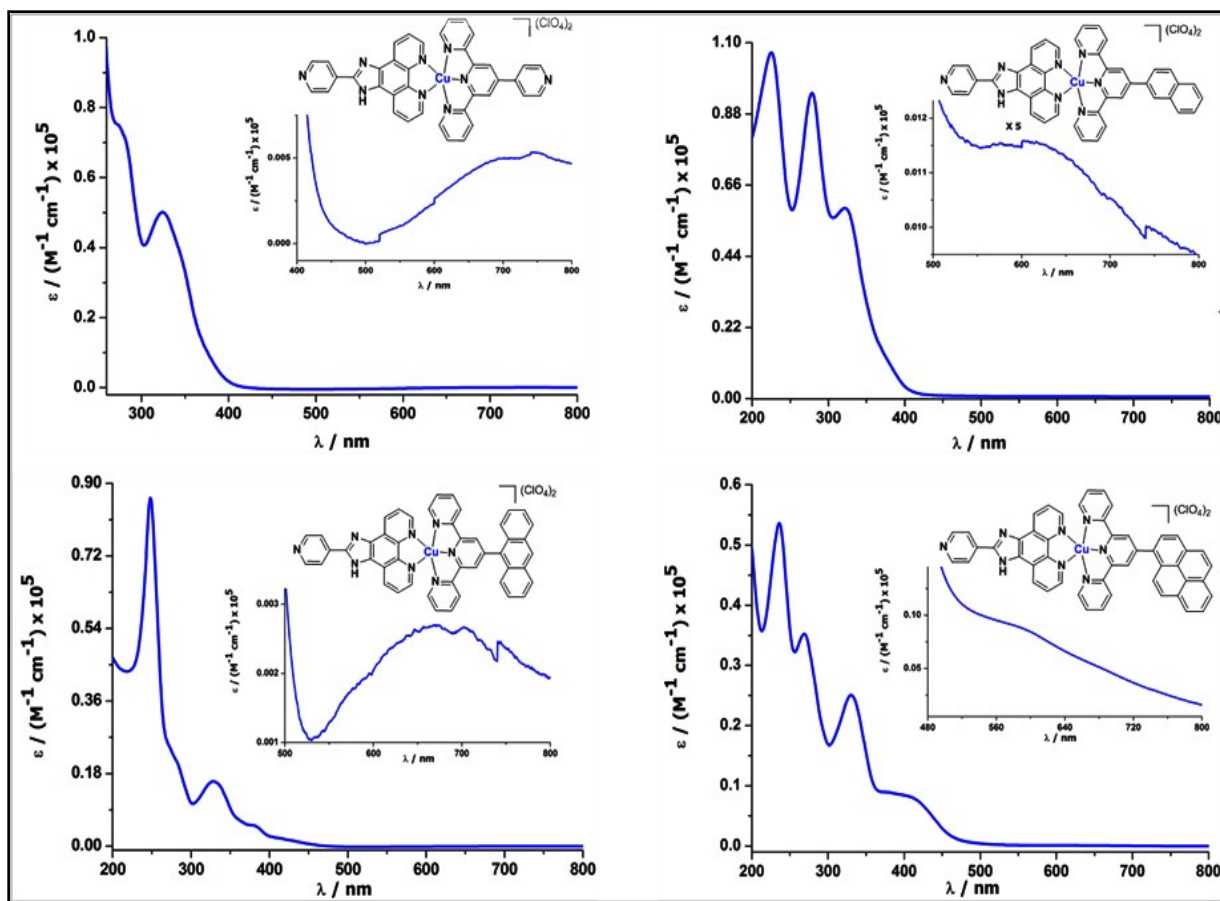


Figure S 10: UV-Vis of terpyridine based ternary copper complexes. TPY-PY-C (Top left, CH_3CN , 10^{-5}M); TPY-NP-C (Top left, CH_3CN , 10^{-5}M); TPY-AN-C (Bottom left, CH_3CN , 10^{-5}M); TPY-PYR-C (Bottom right, CH_3CN , 10^{-5}M). In each figure, the inset shows the d-d bands of the respective complexes.

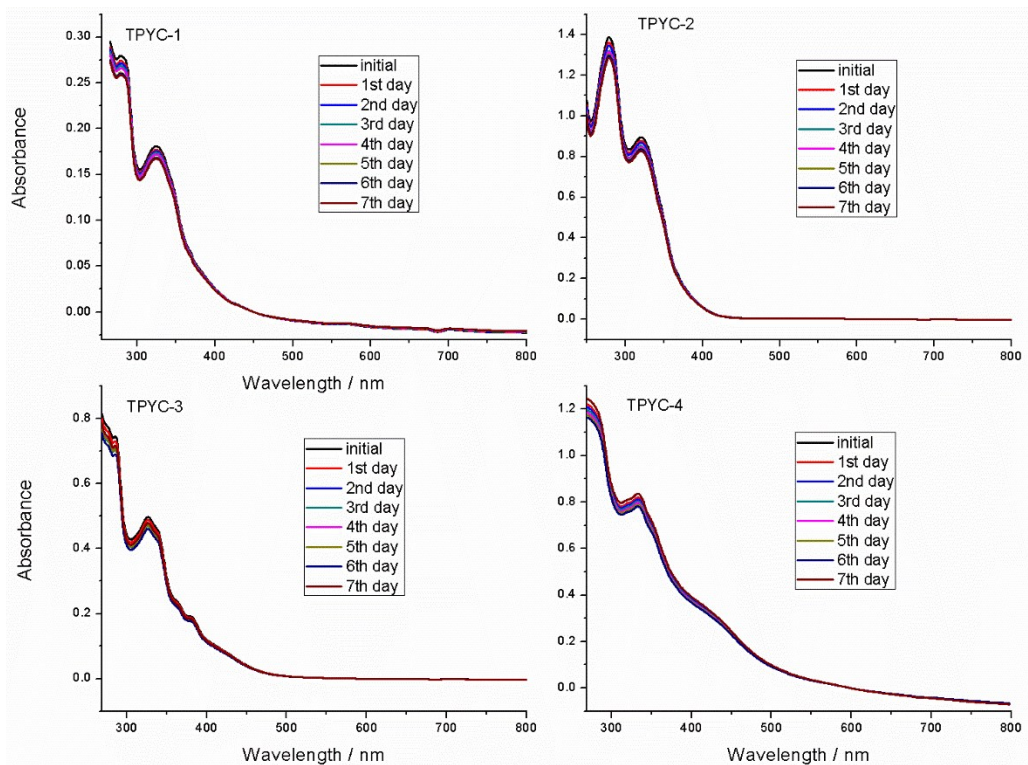


Figure S 11: Figures depicting stability of complexes TPYC-1 to 4 in 10% DMF/tris HCl buffer solution over 7 days. The stability was monitored through UV-vis spectroscopy where no observable changes were observed in the UV-vis spectrum of complexes over 7 days.

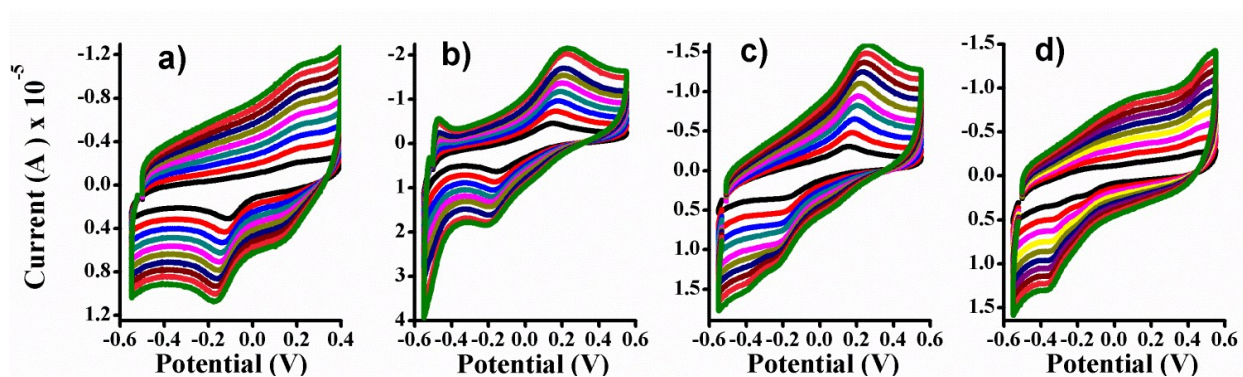


Figure S 12: Cyclic voltammograms of TPYC complexes at increasing scan rate from 100 mV/s to 1000 mV/s. a) TPYC-1; b) TPYC-2; c) TPYC-3; d) TPYC-4.

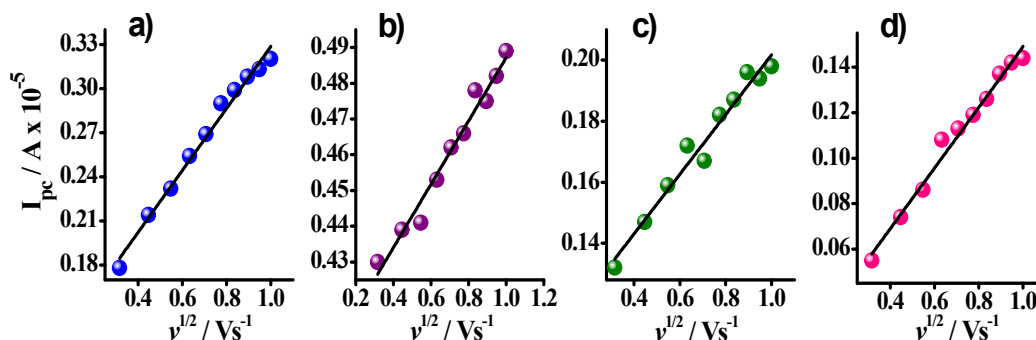


Figure S 13: Plot of I_{pc} vs square root of scan rate for a) TPYC-1 ($R^2 = 0.98$), b) TPYC-2, ($R^2 = 0.97$) c) TPYC-3 ($R^2 = 0.96$) and 4) TPYC-4 ($R^2 = 0.98$). Linear fitting of the data points is indicative of diffusion controlled process.

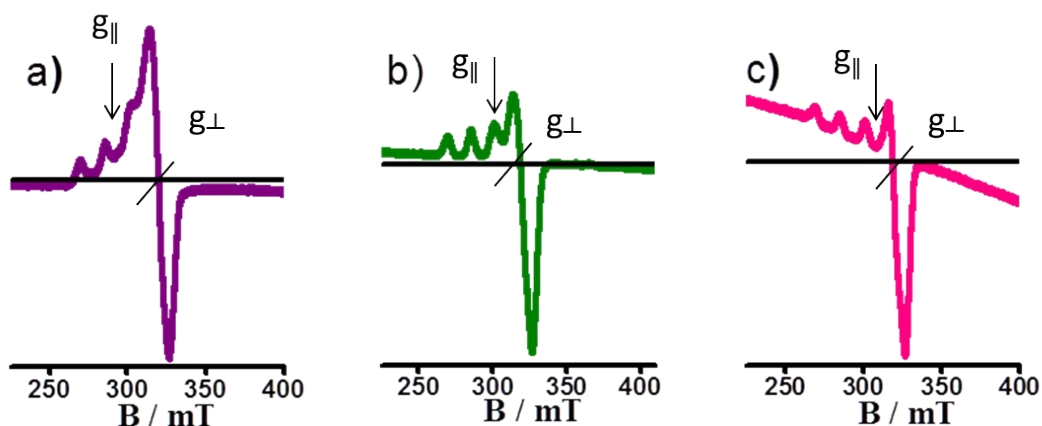


Figure S 14: X-band EPR spectra of a) TPYC-2, b) TPYC-3 and c) TPYC-4 in DMF glass at 77K. Other instrumental conditions same as mentioned for TPYC-1 in the text.

DNA binding, chemical- and photo-cleavage activities.

Mode and extent of binding of complexes TPYC-1 to 4 with DNA was monitored using a combination of UV/Vis and fluorescence spectroscopic techniques. Circular dichroism studies were performed to analyse if any conformational changes were induced into DNA structure upon interaction with complexes. Thermal denaturation studies were performed so as to gauge the stability/instability brought into the DNA structure. All experiments were performed under physiological conditions of

temperature and pH. DNA cleavage activities of these complexes were carried out *via* gel electrophoresis and photographed using Gel-documentation system.

UV/Vis studies. In absorption spectral titrations (AST), fixed aliquots of ct-DNA in 50 mM tris HCl/NaCl buffer (pH = 7.2) were added to 10 μ M (DMF: H₂O :: 1:9 (v/v)) solutions of TPYC-1 to 4 and optical absorption was recorded after 5 minute equilibration time and 200 nm min⁻¹ scan speed, until there were no further alterations in the optical absorption. Equal quantity of ct-DNA was added to the reference side as well so as to nullify the effect of DNA absorption. Interpretation and subsequent calculation of binding parameters from UV/Vis data was followed after due volume corrections. Intrinsic binding constant, K_b was calculated using McGhee von Hippel equation^[7] (1),

$$[\text{DNA}]/(\epsilon_a - \epsilon_f) = [\text{DNA}]/(\epsilon_b - \epsilon_f) + 1/K_b(\epsilon_b - \epsilon_f)\dots\dots(1)$$

where, ϵ_f , ϵ_b , ϵ_a are the molar extinction coefficients of the free complex, of fully bound complex, and at addition of each aliquot of DNA (apparent), respectively. [DNA] is the concentration of ct-DNA in base pairs. ϵ_a can be calculated using $A_{\text{obs}}/[\text{Complex}]$,^[8] where A_{obs} is absorbance of the complex and [Complex] is the dilution corrected concentration of the complex after each addition of aliquot of DNA. Expression of Bard and coworkers^[9] (modified MvH equation) (2) and (3) was used for calculating binding site size, 's' in base pairs.

$$\Delta\epsilon_{af} / \Delta\epsilon_{bf} = (b - (b^2 - 2K_b^2C_t[\text{DNA}]/s)^{1/2})/2K_bC_t\dots\dots(2)$$

$$\text{where } b = 1 + K_bC_t + K_b[\text{DNA}]/2s\dots\dots(3)$$

Number of binding sites per molecule, Γ_{max} could be calculated using equation (4),^[10]

$$\Gamma_{\text{max}} = 1/2s\dots\dots(4)$$

Competitive displacement assays. A solution of 2 mL of 1.3 μM of EB prepared in 50 mM tris HCl/NaCl buffer was excited at 501 nm and emission was recorded at 601 nm. 10 μL aliquots of 300 μM ct-DNA were subsequently added to EB solution resulting in enhancement of fluorescence intensity (measured at same excitation and emission wavelengths), until there were no further changes. The experiment was performed three times under identical conditions and after subtracting the value of the baseline (Tris HCl buffer), the fluorescence value ' F ', at $\lambda_{\text{max}} = 601$ nm was corrected for dilutions using equation **5**.

$$F_{\text{corr}} = F \times (2000 + X) / 2000 \dots \dots \dots (5)$$

where ' F_{corr} ' is the corrected fluorescence value, 2000 is mixture volume in microlitres before DNA addition and X is the volume of DNA solution added. A quantity ' f ' (equation **6**) was used to represent fraction of EB bound to DNA. Scatchard method^[11-13] as described by Healy^[14] was employed for fitting the collected data for three sets within experimental error limits (Fig. 1) (equation **7**).

$$f = (F_{\text{corr}} - F_0 / F_{\text{max(corr)}} - F_0) \dots \dots \dots (6)$$

$$[\text{DNA}] / f = (N / K_{\text{EB}}) \times (1 - f)^{-1} + N \times [\text{EB}] \dots \dots \dots (7)$$

where ' N ' is the number of base pairs per molecule of EB and K_{EB} is EB-DNA binding constant. K_{EB} and ' N ' were calculated to be $1.05 \times 10^7 \text{ M}^{-1}$ and ~ 2.5 base pairs which is well within the error limits of the reported value.

To this EB-Bound DNA solution, increasing aliquots of 1 mM stock solutions of various copper complexes were added in separate experiments, and at similar excitation and emission wavelengths, continuous fluorescence quenching was observed for each complex. Apparent binding constant, K_{app} for complexes were calculated using equation **8**.^[15]

$$K_{\text{EB}} \times [\text{EB}] = K_{\text{app}} \times \text{DC}_{50} \dots \dots \dots (8)$$

where, $[\text{EB}] = 1.3 \mu\text{M}$ and DC_{50} is the concentration of complex at 50 % EB displacement.

To quantitatively correlate fluorescence quenching to the concentration of the quencher, that is, copper complexes, fluorescence data were transformed into Stern–Volmer plots according to Stern–Volmer equation **9** for collisional/dynamic quenching.^[16]

$$F_0 / F = 1 + K_{sv} \times [Q] \dots \dots \dots (9)$$

where F_0 and F are the fluorescence area in the absence and presence of the quencher, $[Q]$ is the ratio of the concentration of the copper complexes to DNA and K_{sv} is the Stern-Volmer quenching constant and is the measure of accessibility of the copper complexes to the EB-DNA intercalating sites.^[17]

Circular dichroism studies. Circular Dichroism (CD) spectrum of the ct-DNA was recorded both in absence and presence of copper complexes. In the CD spectrum of ct-DNA, two conservative bands, one positive absorption band (260 to 280 nm) with $\lambda_{max} = \sim 275$ nm and the negative band at $\lambda_{max} = 245$ nm are observed and are due to the base stacking and the right-handed helicity of B form of DNA, respectively. In other experiments, the concentration of ct-DNA was 100 μ M and of the copper complexes was 10 μ M. CD spectra were recorded after an equilibration time of 5 minutes. Each CD spectrum was collected after averaging over at least 3 accumulations using a scan speed of 100 nm min⁻¹ and a 2s response time. Baseline was recorded with Tris HCl solution and was adjusted in the CD spectra of DNA and DNA + complexes.

Thermal denaturation studies. Individual 0.3 mL solutions containing 130 μ M bp of ct-DNA in 50 mM Tris HCl/NaCl buffer pH 7.2 and 33 μ M of complex solution were placed in 0.50 mL quartz cuvettes. For the calculation of T_m , temperature is increased at a fixed rate of 1 $^{\circ}$ C min⁻¹ and absorbance at $\lambda = 260$ nm is measured after every 0.5 $^{\circ}$ C rise in temperature. As the temperature is increased, absorbance of DNA tends to increase owing to unwinding of ds DNA to ss DNA. DNA melting curves were normalized between 0 and 1 and the first derivative, $\Delta A_{260}/\Delta T$, was

determined using Origin 8.0 graph plotting software, where the T_m value for each melting transition was marked by the maximum of the first derivative plot. Pure ct-DNA melting temperature, $T_m^{\circ} = 77.5$ °C as deduced experimentally.

Chemical nuclease activity. For chemical nuclease activity, 3-mercaptopropionic acid was used as co-reductant. At First, control experiments were performed, where 3-MPA was not added to the samples. Samples were prepared using 10 μM of each of the complex was added to 0.5 μL of pUC19 DNA (from 250 $\mu\text{g}/\text{mL}$ solution). After mixing them using a spinner, the samples were incubated for 1.5 h at 37.5 °C under dark conditions. After incubation, 2 μL of loading buffer, containing 25% bromophenol blue, 0.25% xylene cyanol, and 30% glycerol, was added to each sample and spinned to mix. Gel electrophoresis was performed using BioRAD PowerPac Basic and BioRAD mini sub-cell GT with 10 μL of incubated sample under optimized conditions of 0.8 % agarose gel, potential was maintained at 40V, 2h running time and dark conditions in 1X tris acetate-EDTA (TAE) buffer. The bands were photographed using BioRAD molecular imaging ChemiDoc XRS+. Then, concentration variation study is performed for each of the complex (for concentration optimization) in which 0.5 μL of puc19 DNA was taken in separate vials using eppendorf and 5 to 15 μM of each of the complex were added in separate vials. Based on concentration optimization studies, 10 μM of the respective complex was mixed with 1 μL of puc19 DNA for all DNA cleavage studies. For chemical nuclease activity, 1.25 μL of 5 mM of 3-mercaptopropionic acid (3-MPA) was added to it and total volume was made to be 20 μL by adding 50 mM tris HCl/NaCl buffer. After mixing them using a spinner, the samples were incubated for 1.5 h at 37.5 °C under dark conditions. Gel-electrophoresis was performed under similar conditions as mentioned above.

Photonuclease activity. Samples for photonuclease activity were prepared in glass vials in the manner similar to chemical nuclease activity but without 3-MPA. Samples were irradiated with UV-A light (365 nm, 12 W) for 0.5 h and were

incubated at 37.5 °C for 1 h under dark conditions. Gel-electrophoresis was performed under similar conditions as mentioned above.

Mechanistic experiments. Number of control experiments were performed by using 5 µL of 5 mM each of NaN₃ (¹O₂ quencher),^[18] D₂O (¹O₂ lifetime enhancer),^[19] DMSO (OH· Scavenger),^[20] KI (O₂²⁻ and OH· Scavenger).^[21, 22] These were added prior to the addition of the respective complex. Gel-electrophoresis was performed under similar conditions as mentioned above.

Following the above procedure, chemical and photo nuclease activity of the **TPYC-1** to **4** was ascertained and percent of DNA cleavage (C) was calculated using equation 10.^[23]

$$C = ([\text{Form II}] + 2[\text{Form III}]) / ([\text{Form I}] + [\text{Form II}] + 2[\text{Form III}]) \dots \dots \dots (10)$$

where Form I represents supercoiled DNA (SC DNA), Form II represents nicked circular DNA (NC DNA) and Form III represents Linear DNA. Corrections were made to 'C' for presence of low level of nicked DNA in uncut plasmid and also low level of affinity of EB binding to supercoiled compared to nicked circular and linear forms of DNA.^[24] % DNA cleavage given in this study for each set of experiment is the mean of three separate experiments performed under similar conditions.

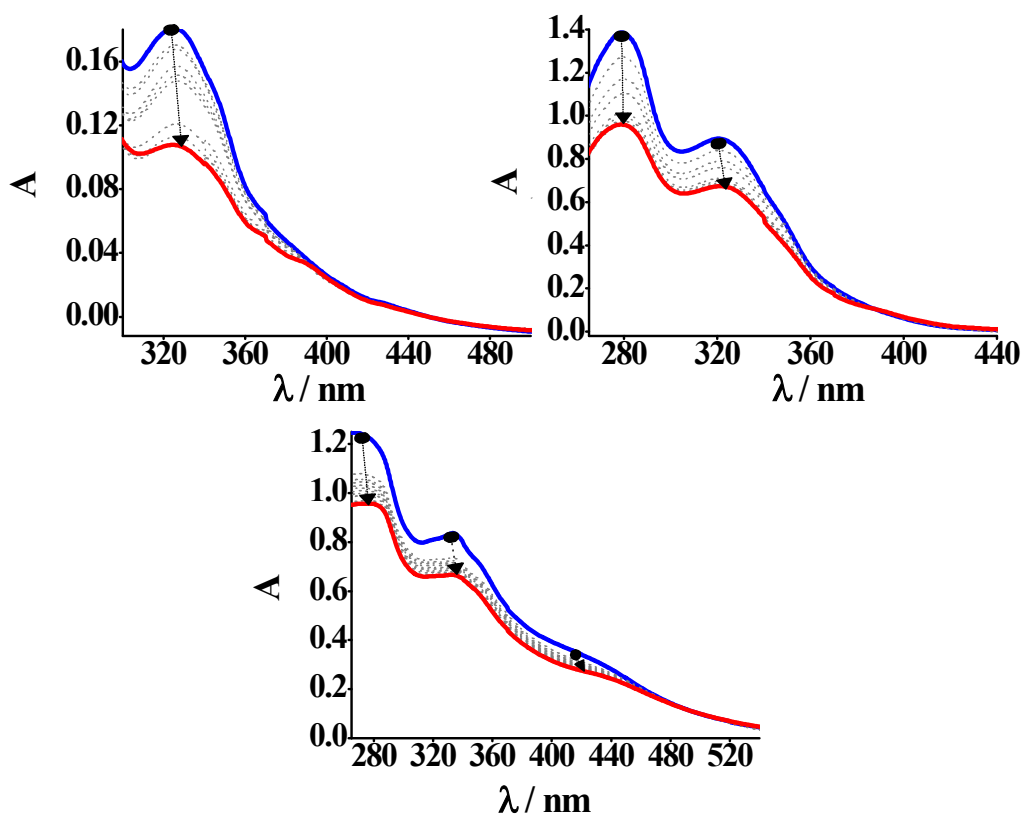


Figure S 15: Absorption spectral titrations of TPYC-1 (Top Left); TPYC-2 (Top Right); TPYC-4 (Bottom) against ct-DNA. Concentration of each complex is 10 μM .

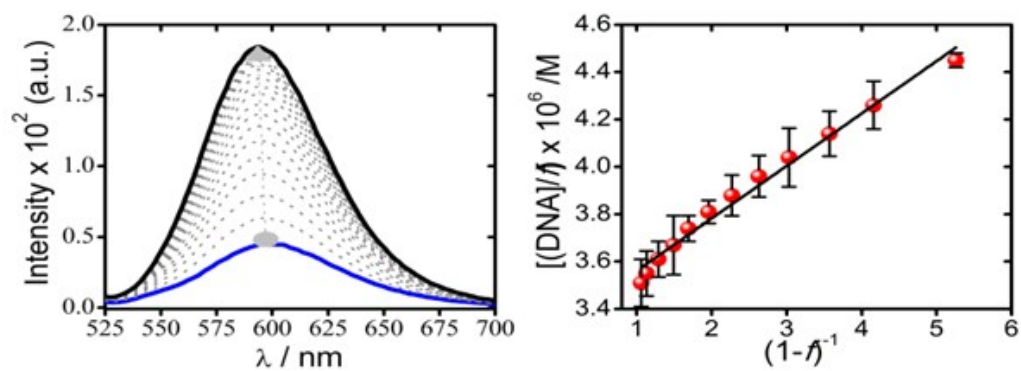


Figure S 16: (Left) Blue line: fluorescence of EB in tris HCl buffer solution; To this EB solution, aliquots of DNA were added resulting in gradual increase in fluorescence with saturation shown by black line. (Right) Scat chard plot for calculating K_{EB} (linear least square fitting; $R^2 = 0.99$).

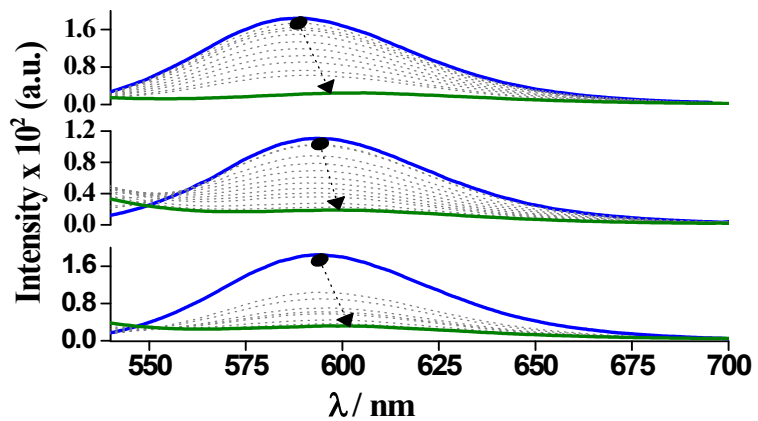


Figure S 17: Addition of TPYC complexes to EB bound DNA. (Top) TPYC-1; (Middle) TPYC-2I (Bottom) TPYC-4.

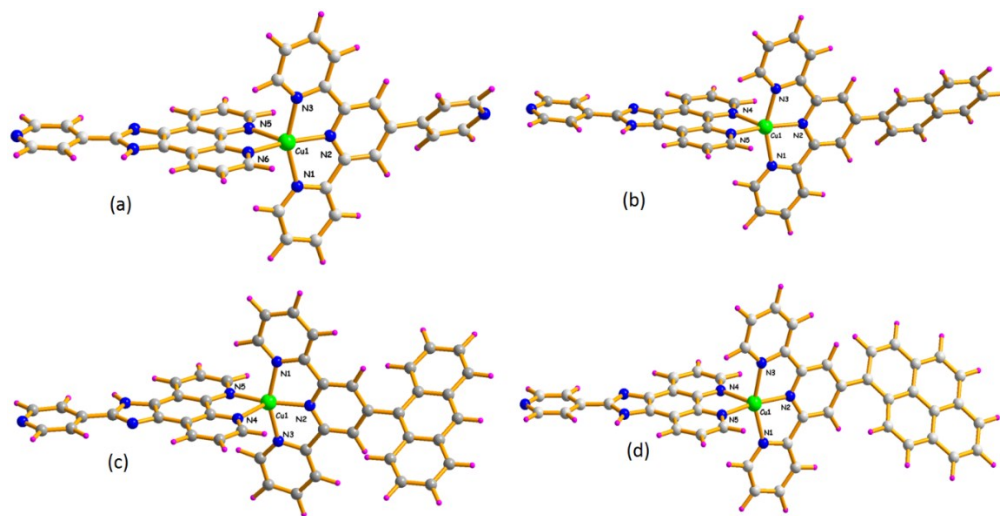


Figure S 18: DFT optimized structure of complexes. (a) TPYC-1; (b) TPYC-2; (c) TPYC-3; (d) TPYC-4.

Table S 1: EPR spectral data for complexes TPYC-1 to 4

Comple x	g_{\parallel}	g_{\perp}	A_{\parallel}^a	$g_{\parallel} / A_{\parallel}$	G	α^2
TPYC-1	2.171	2.050	168	129	3.40	0.6941
TPYC-2	2.169	2.044	170	127	3.84	0.6961
TPYC-3	2.168	2.051	160	135	3.29	0.6709
TPYC-4	2.174	2.052	181	120	3.29	0.7357

^a $A_{\parallel} \times 10^{-4} \text{ cm}^{-1}$

Table S2: Selected bond lengths (\AA) for complexes 1 and 2 from DFT data.

	TPYC-1	TPYC-2	TPYC-3	TPYC-4
Cu-N1	2.1034	2.1045	2.1063	2.1013
Cu-N2	1.9756	1.9666	1.9687	1.9629
Cu-N3	2.1035	2.1042	2.1048	2.1026
Cu-N4	-	2.2559	2.2572	2.2612
Cu-N5	2.2502	2.0445	2.0474	2.0509
Cu-N6	2.0410	-	-	-

Table S3: Selected bond angles from DFT data

	TPYC-1	TPYC-2	TPYC-3	TPYC-4
N1-Cu-N2	78.863	78.905	78.887	78.980
N1-Cu-N5	98.938	99.611	99.628	99.720
N1-Cu-N6	99.676	-	-	-
N1-Cu-N3	156.103	156.219	156.414	156.658
N2-Cu-N5	116.566	165.266	164.288	164.491
N2-Cu-N4	-	116.318	117.364	117.353
N4-Cu-N1	-	98.792	98.079	98.601
N3-Cu-N4	-	98.648	99.106	98.235
N4-Cu-N5		78.416	78.347	78.155
N2-Cu-N6	164.785	-	-	-
N2-Cu-N3	78.858	78.923	78.912	78.968
N3-Cu-N5	98.660	99.631	99.571	99.469
N3-Cu-N6	99.538	-	-	-
N5-Cu-N6	78.649	-	-	-

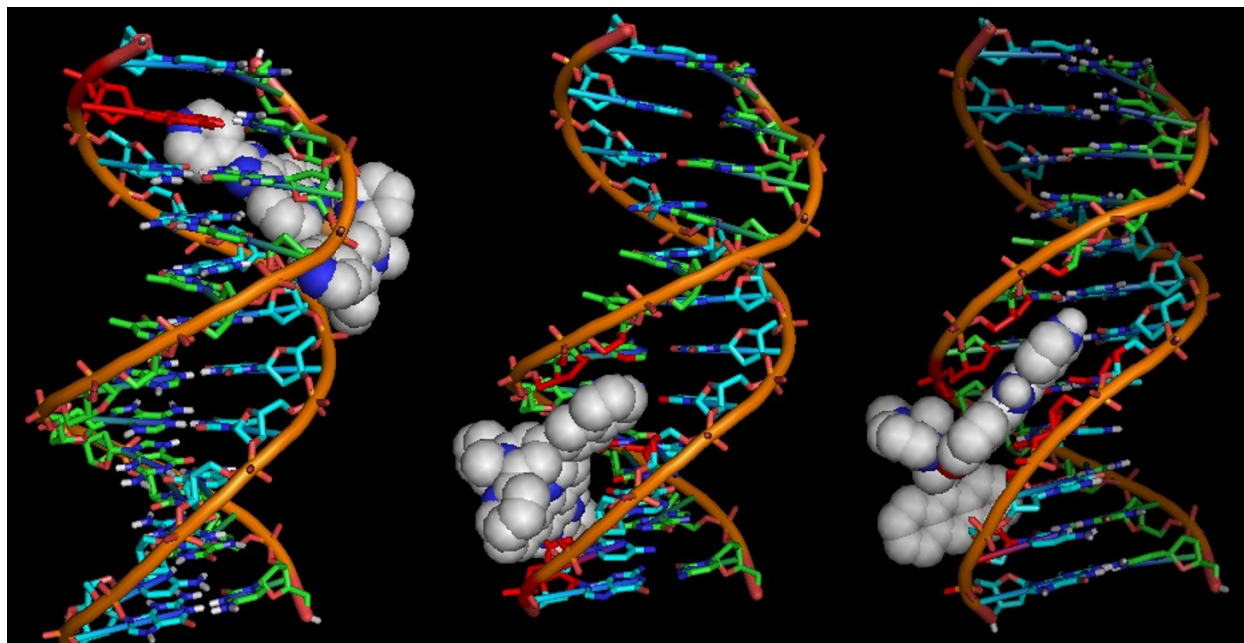


Figure S 19: Docked structure of (a) TPYC-1; (b) TPYC-2; (c) TPYC-3 with d(CGCGAATTCGCG) strands of DNA.

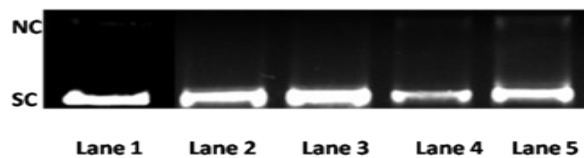
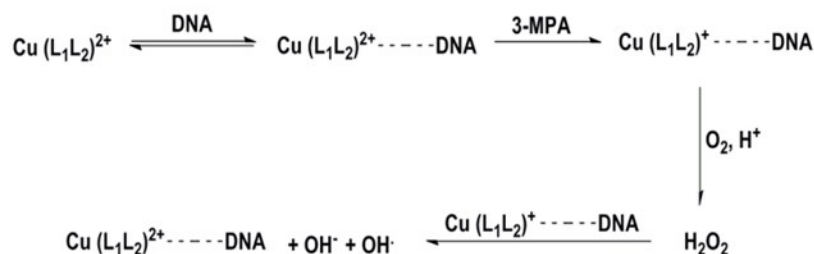
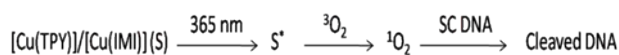


Figure S 20: DNA cleavage activity of all complexes without the addition of 3-MPA. Lane 1: DNA control; Lane 2 DNA + TPYC-1; Lane 3: DNA + TPYC-2; Lane 4: DNA + TPYC-3; Lane 5: DNA + TPYC-4. % nicked DNA is pretty low at $\sim 4-5\%$ in three separate experiments for each of the complex.



Scheme S 1: Proposed mechanism for generation of ROSs through complexes and subsequent DNA cleavage.



Scheme S 2: Proposed mechanism for generation of singlet oxygen and photo-induced DNA cleavage activity.

References:

1. N. Noshiranzadeh, A. Ramazani, A. Morsali, A. D. Hunter, M. Zeller, *Inorg. Chim. Acta*, 2007, **360**, 3603.
2. J. F. Michalec, S. A. Bejune, D. G. Cuttell, G. C. Summerton, J. A. Gertenbach, J. S. Field, A. J. Haines, D. R. McMillin, *Inorg. Chem.*, 2001, **40**, 2193.
3. M. N. Patel, D. S. Gandhi, P. A. Parmar, H. N. Joshi, *J. Coord. Chem.*, 2012, **65**, 1926.
4. W. Leslie, R. A. Poole, P. R. Murray, L. J. Yellowlees, A. Beeby, J. A. G. Williams, *Polyhedron*, 2004, **23**, 2769.
5. N. N. Sergeeva, M. D. Marechal, G. Vaz, A. M. Davies, M. O. Senge, *J. Inorg. Biochem.*, 2011, **105**, 1589.
6. R. D. Crouch, J. L. Howard, J. L. Zile, K. H. Barker, *J. Chem. Edu.*, 2006, **83**, 1658.
7. J. D. McGhee, P. H. V. Hippel, *J. Mol. Biol.*, 1974, **86**, 469.
8. E. Sundaravadivel, M. Kandaswamy, B. Varghese, *Polyhedron*, 2013, **61**, 33.
9. M. T. Carter, M. Rodriguez, A. J. Bard, *J. Am. Chem. Soc.*, 1989, **111**, 8901.
10. W. Chen, N. J. Turro, D. A. Tomalia, *Langmuir*, 2000, **16**, 15.
11. H. G. Weder, J. Schildknecht, R. A. Lutz, P. Kesselring, *Eur. J. Biochem.*, 1974, **42**, 475.
12. J. G. Norby, P. Ottolenghi, J. Jensen, *Anal. Biochem.*, 1980, **102**, 318.
13. K. Zierler, *Trends Biochem. Sci.*, 1989, **14**, 314.

14. E. F. Healy, J. Chem. Edu., 2007, **84**, 1304.
15. M. Lee, A. L. Rhodes, M. D. Wyatt, S. Forrow, J. A. Hartley, Biochemistry, 1993, **32**, 4237.
16. J. R. Lakowicz, Principles of Fluorescence Spectroscopy, 2nd edn., Kluwer Academic/Plenum Publishers, 1999.
17. D. Sarkar, P. Das, S. Basak, N. Chattopadhyay, J. Phys. Chem., 2008, **112**, 9243.
18. B. W. Henderson, T. Dougherty, J. Photochem. Photobiol., 1992, **55**, 145.
19. J. R. Harbour, S. L. Issler, J. Am.Chem. Soc., 1982, **104**, 903.
20. P. B. Merkel, R. Nilsson, D. R. Kearns, J. Am. Chem. Soc., 1972, **94**, 1030.
21. J. E. Repine, J. W. Eaton, M. W. Anders, J. R. Hoidal, R. B. Fox, J. Clin. Invest., 1979, **64**, 1642
22. J. E. Repine, O. W. Pfenninger, D. W. Talmage, E. M. Berger, D. E. Pettijohn, Proc. Natl. Acad. Sci. USA, 1981, **78**, 1001.
23. M. Mariappan, B. G. Maiya, Eur. J. Inorg. Chem., 2005, 2164.
24. D. R. Smith, *Agarose Gel Electrophoresis, Basic DNA and RNA Protocols, Methods in Mol. Biol.*, 1996, **58**, 17.